

Optical configuration of a horizontal-switching liquid-crystal cell for improvement of the viewing angle

Joun-Ho Lee, Hyunchul Choi, Seung Hee Lee, Jae Chang Kim, and Gi-Dong Lee

We propose an optical configuration of a horizontal-switching liquid-crystal cell, consisting of a splayed liquid-crystal cell and uniaxial films, to improve the viewing angle characteristics by compensating for the phase dispersion in a diagonal direction. The optical design of the proposed configuration was performed on a Poincaré sphere with geometric calculations. By fabricating in-plane switching cells with the introduced configuration, we demonstrated their optical performances. As a result, we found that the diagonal viewing angle of the proposed horizontal-switching cell could be increased by 80% compared to a symmetrical viewing cone. © 2006 Optical Society of America

OCIS codes: 230.3720, 230.0230, 220.0220.

1. Introduction

In general, horizontal-switching liquid-crystal (LC) cells such as the super-in-plane-switching (S-IPS) mode and the fringe field switching (FFS) mode show intrinsically excellent viewing angle characteristics. Therefore they have been used in large size displays such as monitors and especially TV applications. In spite of the excellent viewing angle performance, the contrast ratio in the oblique diagonal direction becomes lower because the effective angle between the absorption axis of a polarizer and an analyzer in the diagonal direction increases in proportion to the observation direction.^{1–3}

To improve the viewing angle characteristics of the horizontal-switching cell in the diagonal direction, several types of optical configuration of the IPS LC cell have been proposed. Chen *et al.*⁴ have shown the combination of an A plate with a +C plate, and Saitoh *et al.*⁵ have shown a configuration using one biaxial film (NEZ film).⁵ Ishinabe *et al.* have also shown a

configuration using two biaxial films.⁶ The optical configuration using biaxial films provides good optical characteristics by blocking the light leakage in the dark state in all directions, but it would be hard to control uniformity for a large-sized LC display.

Here we propose an optical configuration of a horizontal-switching LC cell for not only wide viewing angles in all directions but also symmetrical viewing characteristics. The proposed optical configuration consists of the splayed horizontal-switching LC cell and uniaxial films, two A plates and a +C plate. The splayed LC cell can provide symmetry in all viewing directions and uniaxial films can allow the LC cell to be uniform. Optimization of the optical retarders for the wide wavelength region has been performed on a Poincaré sphere by applying a spherical trigonometry method.⁷ To verify the calculation, we measured the viewing angle of the proposed optical configuration of the horizontal-switching cell experimentally and compared that with a conventional horizontal-switching cell. As a result, we found that the contrast ratio of the proposed horizontal-switching cell can be increased 80% compared to the symmetrical viewing cone.

2. Light Leakage of Horizontal-Switching Liquid-Crystal Cells in a Diagonal Direction in the Dark State

Figure 1 shows the asymmetric viewing cone of the conventional horizontal-switching cell. As shown in Fig. 1, a horizontal-switching cell can show a very wide viewing angle in the horizontal and vertical directions. On the other hand, the optical contrast in the diagonal direction deteriorates due to light leakage in the dark state. Light leakage in the dark state could occur for several reasons.

J.-H. Lee and H.-C. Choi are with the LG Philips LCD, 642-3 Jinpyung-dong, Gumi-city, Kyungbuk 730-350, South Korea. S. H. Lee is with the School of Advanced Materials Engineering, Chonbuk National University, Chonbuk 561-756, South Korea. J.-C. Kim, as well as J.-H. Lee, is with the Department of Electronics Engineering, Pusan National University, Pusan 609-735, South Korea. G.-D. Lee (gdlee@dau.ac.kr) is with the Department of Electronics Engineering, Dong-A University, Pusan 604-714, South Korea.

Received 11 January 2006; revised 17 May 2006; accepted 23 May 2006; posted 24 May 2006 (Doc. ID 67164).

0003-6935/06/287279-07\$15.00/0

© 2006 Optical Society of America

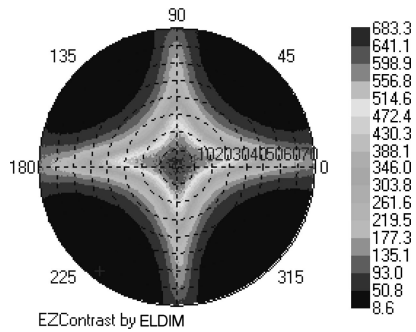


Fig. 1. Measured isocontrast contour of the conventional horizontal-switching cell (measured by ELDIM).

The first is the geometric issue of *O*-type polarizers, which means they transmit the ordinary waves of incident light. In crossed *O*-type polarizers, the effective angle between the absorption axis of the polarizer and the analyzer increases as the oblique incident angle in the diagonal direction increases. Figure 2 shows a change in the effective absorption angle of the two crossed polarizers. In oblique incidence, the absorption angle of the polarizers deviates angle δ from normal incidence at an azimuth angle of 45° . The light leakage in the dark state due to a change in the effective angle between the two polarizers can be effectively described on the Poincaré sphere.⁸ A numerical approach to obtain the deviation angle δ is as shown below.

If we assume that the birefringence is small (i.e., $|n_e - n_o| \ll n_e, n_o$) and the refractive indices are well

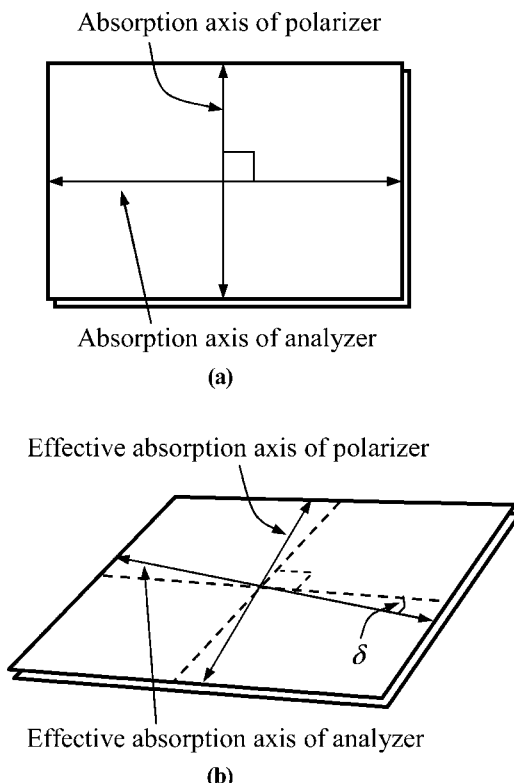


Fig. 2. Change in the effective angle of the absorption angle of the crossed polarizers: (a) normal observation, (b) oblique observation.

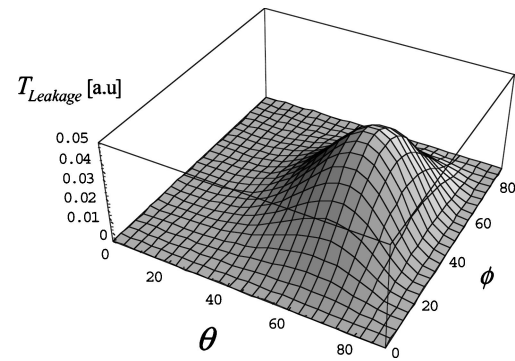


Fig. 3. Calculated transmission of light passing through a pair of crossed ideal *O*-type polarizers.

matched at the interface, we can assume that both ordinary and extraordinary waves propagate along the same direction. Generally, the optical axis of polarizer and analyzer is parallel to the plane of glass. Then, we can define angle δ in terms of ϕ_c and θ_o as shown below⁹:

$$\delta = \sin^{-1} \left\{ \sin \left[\frac{\cos \theta_o \sin \phi_c}{(1 - \sin^2 \theta_o \sin^2 \phi_c)^{1/2}} \right] \right\}, \quad (1)$$

where ϕ_c is the azimuth angle of the optical axis of the polarizer and θ_o is the polar angle of the incident light for the LC cell layer, respectively.

Light leakage T_{leakage} in terms of ϕ_c and θ_o in the crossed polarizers can also be easily obtained⁹:

$$T_{\text{leakage}} = \frac{1}{8} T^4 \frac{\sin^2 2\phi \sin^4 \theta_o}{(1 - \cos^2 \phi \sin^2 \theta_o)(1 - \sin^2 \phi \sin^2 \theta_o)}. \quad (2)$$

The factor T^4 accounts for the Fresnel transmission of light through the four interfaces of the two polarizers. ϕ is the azimuth angle and Fig. 2 shows the calculated transmittance of the light passing through a pair of crossed ideal *O*-type polarizers. From Fig. 3, we can confirm that crossed *O*-type polarizers exhibit the highest light leakage in a diagonal direction ($\phi = 45^\circ$).

Then we consider the light leakage from the change of the retardation of each optical plate with oblique incident direction. The effective retardation of the *A* plate, the horizontal-switching LC cell, and the *C* plate in the oblique incident angle can be described as⁹

$$\Gamma_a = \frac{2\pi}{\lambda} d \left[n_e \left(1 - \frac{\sin^2 \theta \sin^2 \phi}{n_e^2} - \frac{\sin^2 \theta \cos^2 \phi}{n_o^2} \right)^{1/2} - n_o \left(1 - \frac{\sin^2 \theta}{n_o^2} \right)^{1/2} \right], \quad (3a)$$

$$\Gamma_C = \frac{2\pi}{\lambda} \frac{d}{\cos \theta_o} \left[\sqrt{\frac{n_o^2 n_e^2}{n_o^2 \sin^2 \theta_o + n_e^2 \cos^2 \theta_o}} - n_o \right]. \quad (3b)$$

Γ_a and Γ_c represent the retardation of the A and C plates at the oblique incidence, d represents the thickness, θ represents the polar angle of incident light, and n_e, n_o represent the refractive indices of the LC. From Eqs. (3) we can calculate that the retardation of the to A plate and horizontally aligned LC cell is changed to within 5% even though the oblique incident angle at the diagonal direction increases to 90° , so that the effect of change of the retardation on the light leakage might be very small. On the other hand, we can calculate that the C plate may have a large change in retardation compared to the A plate from Eqs. (3).

The last issue is phase dispersion of the refractive index along the wavelength. In general, the dispersion is also dependent on the material property. The polarization states of the three primary colors (R , G , and B) differ from each other after passing through the LC cell and retardation films because of the different materials and wavelength dispersion. To get less light leakage in the dark state and achromatic black picture, the dispersion property along the wavelength should be effectively eliminated. We introduce a geometric design method on the Poincaré sphere to eliminate the dispersion property.

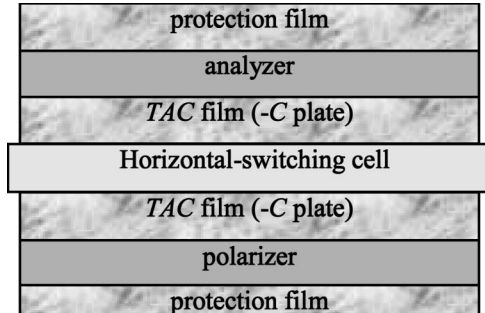
3. Geometric Design of the Horizontal-Switching Cell on the Poincaré Sphere

A. Effective Optical Axis of the Retarder in the Oblique Incidence

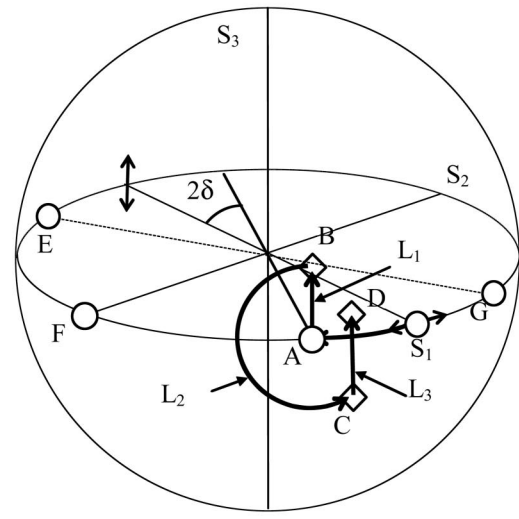
In the oblique incidence, the optical axis of the retardation film will also move to another position, which is similar to the polarizer, as we mentioned above. The effective angle of the optical axis of the A plate is exactly the same as that of the polarizer. Therefore the optical axis will move to δ from the angle of normal incidence, as shown in Fig. 2(b). In contrast, the effective slow and fast axes of the negative C and $+C$ plates move to 90° with respect to the projected angle of the incident k vector, respectively. Therefore we can easily calculate the centered position for rotation on the Poincaré sphere by each uniaxial film.

B. Polarizations in the Conventional Horizontal-Switching Liquid-Crystal Cell

The conventional horizontal-switching cell consists of a homogeneous LC cell and two tri-acetyl-cellulose (TAC) films ($-C$ plate $\equiv -42$ nm) on upper and lower polarizers as shown in Fig. 4(a). Figure 4(b) shows the polarization state of the light obliquely passing through the cell in the diagonal direction on the Poincaré sphere. Oblique incident light in the diagonal direction will have a deviated polarization angle δ compared to normal incident light, so that the polarization position of the polarizer will deviate with 2δ from S_1 , which is the polarization state of the polarizer in a normal direction. Therefore the start position of the oblique incident light is position A , as shown in Fig. 4(b). Then the light passing through the



(a)



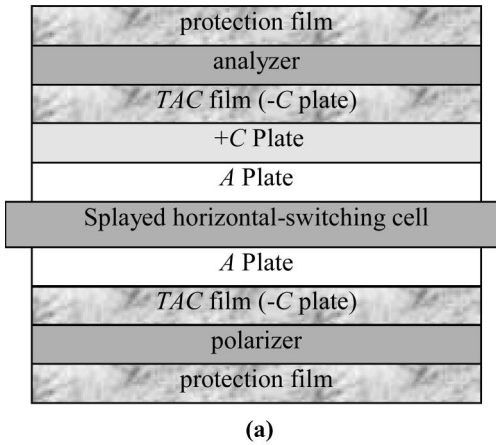
(b)

Fig. 4. Optical configuration of the conventional horizontal-switching LC cell and polarization state of the oblique incident light in the LC cell: (a) optical structure, (b) polarization path on the Poincaré sphere. L_1 , L_2 , and L_3 represent the transfer path of the polarization by the lower TAC, the cell, and the upper TAC film, respectively.

lower TAC film possesses polarization position B along the circle path L_1 , which is centered at point F . Next, the light will move to the C position along the circle path L_2 by experiencing the horizontal cell. Finally, the upper TAC film will make the polarization state D from C with path L_3 again. From Fig. 4(b) we can observe quite different lengths from the polarization state D in front of the output polarizer to output polarizer G . Therefore we can assume that the deviation between D and G will cause serious light leakage in the dark state.

C. Optical Principle and Optimization of the Proposed Horizontal-Switching Liquid-Crystal Cell

Compensation for the deviated polarization by oblique incidence can be achieved by adding several retarders to the conventional mode. Figure 5(a) shows the proposed optical configuration of the horizontal-switching cell, which can improve the viewing angle in the diagonal direction. The optical configuration of the proposed LC cell consists of two A plates, a $+C$ plate, and a splayed horizontal-switching cell. The optical axis



(a)

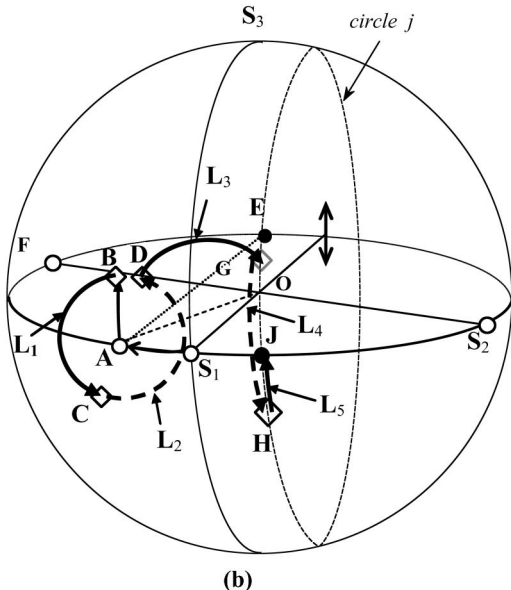


Fig. 5. Optical configuration of the proposed horizontal-switching LC cell and the polarization state of the oblique incident light in the LC cell: (a) optical structure, (b) polarization path on the Poincaré sphere.

of the lower A plate and the horizontal-switching cell is aligned parallel with the absorption axis of the incident polarizer, and the optical axis of the upper A plate is aligned along that of the absorption axis of the analyzer. An improved optical polarization path of the proposed cell is described on the Poincaré sphere as shown in Fig. 5(b). The application of the Poincaré sphere is particularly simple as it lends itself to graphic analysis by spherical trigonometry. Optimization of the optical configuration in this paper has been performed at the diagonal direction, $\phi = 45^\circ$ because the light leakage in the dark state is maximized at $\phi = 45^\circ$.

In the proposed optical configuration, the polarization state in front of the output polarizer can coincide with the absorption axis of the output polarizer through five-paths (L_1-L_5). The polarization of light passing through the lower A plate and the horizontal-switching cell moves to position D along the circle path L_1 and L_2 . The polarization of the light ap-

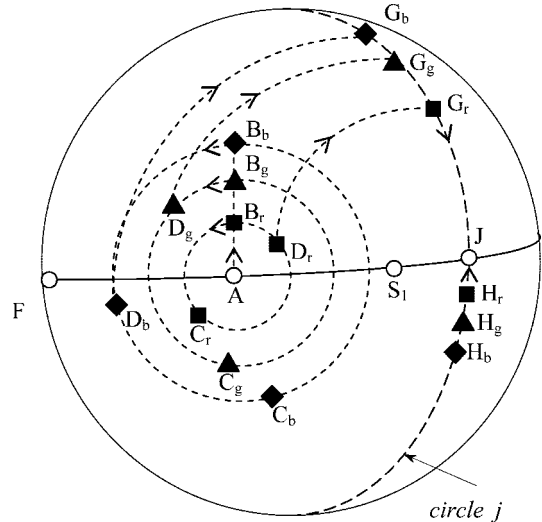


Fig. 6. Polarization state of the light passing through the proposed horizontal-switching cell on the Poincaré sphere in the tri-stimulus wavelengths R , G , and B .

proaches the position G along the circle path L_3 , which is centered at point J because the optical axis of the upper A plate is aligned parallel with the absorption axis of the analyzer. The polarization state of the light will rotate to H along path L_4 on circle j by passing through the $+C$ plate, and, finally, the polarization state will reverse rotate to J along path L_5 on circle j because the TAC film exhibits negative birefringence. Position J is exactly matched with the opposite position of the polarization state of analyzer E . The process of the proposed optical configuration effectively moves to the polarization position of the output polarizers in the oblique incident direction, so that it clearly provides blocking of light leakage in the dark state.

However, for the best dark state, we should consider phase dispersion of the LC cell because the proposed configuration should satisfy the above principle along the range of the entire wavelength so that we need to optimize the retardation value of the two A plates and a single $+C$ plate. Elimination of phase dispersion represents the coincidence of the polarization states among R (633 nm), G (546 nm), and B (436 nm) wavelength on the Poincaré sphere in front of the output polarizer. The process for removing the dispersion on the sphere is described below.

D. Elimination of Phase Dispersion for the Proposed Configuration

Figure 6 shows the optical principle of the proposed horizontal-switching cell to remove the phase dispersion through the wavelengths R , G , and B on the Poincaré sphere. To gather the polarization positions on the entire wavelength to position J , we have to satisfy two conditions as below. The first is that the polarization positions of each wavelength passing through the upper A plate should be on circle j as shown in positions G_b , G_g , and G_r in Fig. 6. The sub-

script of the letter for each position represents the position of each R , G , and B wavelength. The aligned polarizations of the entire wavelength on circle j can be gathered by adjusting the retardation of the upper $+C$ plate.

The second condition to optimize is for control so that the retardation of the $+C$ plate is the same as with the phase dispersion of the TAC film before the light passes the TAC film.

In Fig. 6, ■ represents the polarization at the longest wavelength R , ▲ represents the polarization at the middle wavelength G , and ♦ represents the polarization at the shortest wavelength B . For the calculation, we assume that the TAC film has flat material dispersion, because it has very small retardation.

To satisfy the first condition, we need to calculate angles $\angle D_r J G_r$, $\angle D_g J G_g$, and $\angle D_b J G_b$, which mean retardations of the upper A plate along the three wavelengths. Positions D_r , D_g , and D_b are also perfectly dependent on the dispersion of the retardations of the lower TAC, A plate, and the cell. The angles $\angle D_r J G_r$, $\angle D_g J G_g$, and $\angle D_b J G_b$ can be achieved by using trigonometry on the Poincaré sphere. Here, to obtain the three trigonometric angles $\angle D_r J G_r$, $\angle D_g J G_g$, and $\angle D_b J G_b$, we define new positions D'_r , D'_g , and D'_b , which are the projected positions on the equator as seen from Fig. 7, because $\angle D_r J G_r = \pi/2 \pm \angle D_r J D'_r$, $\angle D_g J G_g = \pi/2 \pm \angle D_g J D'_g$, and $\angle D_b J G_b = \pi/2 \pm \angle D_b J D'_b$. The angle $\angle D_r J D'_r$ in each wavelength can be directly achieved by calculating the rotation length of $\text{arc}(DD')$ and $\text{arc}(D'J)$ in each wavelength:

$$\begin{aligned} \Gamma^{U-A} &= \angle D_r J G_r = \frac{\pi}{2} + (-1)^i \angle D_r J D'_r \\ &= \frac{\pi}{2} + (-1)^i \sin^{-1} \left\{ \frac{\sin[\text{arc}(DD')]}{\sin[\text{arc}(D'J)]} \right\}, \end{aligned}$$

where

$$\begin{aligned} \text{arc}(D'J) &= \cos^{-1}\{\cos[\text{arc}(DD')]\cos[\text{arc}(D'J)]\}, \\ \text{arc}(D'J) &= 4\delta + (-1)^j \text{arc}(AD') \\ &= 4\delta + (-1)^j \sin^{-1} \left(\frac{\tan[\text{arc}(DD')]}{\tan\{(-1)^k[\Gamma^{A+\text{cell}} - (2 + (-1)^j/2)\pi]\}} \right), \\ \text{arc}(DD') &= \sin^{-1} \{(-1)^i \cos\Gamma^{A+\text{cell}} \sin[\text{arc}(AB)]\}, \\ \text{arc}(AB) &= \sin^{-1}(\sin \Gamma^{\text{TAC}} \cos 2\delta), \quad i, j, k, l = 1 \text{ or } 2, \end{aligned} \quad (4)$$

where, Γ^{TAC} represents the retardation of the lower TAC film, $\Gamma^{A+\text{cell}}$ represents the summation of retardation of the lower A plate and the cell, and Γ^{U-A} represents the retardation of the upper A plate. We

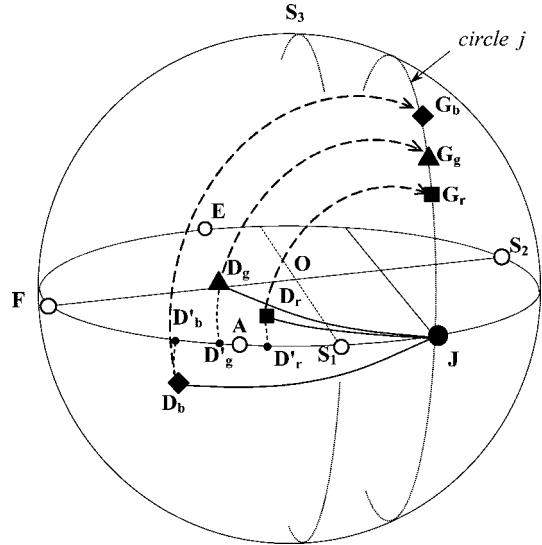


Fig. 7. Polarization state of light after passing through the upper A plate.

handled summed retardation of the lower A plate and the cell because the optical axis of the lower A plate and the cell align to the same angle. In addition, we assume that we already know the dispersion of the LC cell and do not change it for optical performance. Therefore the calculated $\Gamma^{A+\text{cell}}$ can appear as the retardation of the lower A plate.

Equation (4) is applied along the range of the entire wavelength. Therefore we can fix the desired wavelength to circle j on the Poincaré sphere by controlling the retardation of the two A plates and the cell through three wavelengths. Integers i , j , k , and l are dependent on the positions of the R , G , and B wavelengths after passing through the cell. This implies that the wavelength dispersion is dependent on the retardation of the A plate and the cell.

The second condition for removing the phase dispersion of the cell can be performed on circle j . After passing through the upper A plate, the light will experience the $+C$ plate and the TAC film in the upper side. During travel through the two films, the final positions of the polarization state of the light should be coincident to the same position. Therefore optimization of the $+C$ plate is dependent on the retardation value of the TAC film of the polarizer. The simple process for the optimization is illustrated as follows: Fig. 8 shows the polarization state of the light passing through the $+C$ plate and the last TAC film. The positions G_r , G_g , and G_b represent the dispersed polarization state of the light in front of the $+C$ plate with the fast axis OF . To get an achromatic color performance in the dark state, the polarization state of the light passing through the $+C$ plate must move from G_r , G_g , and G_b to H_r , H_g , and H_b , which are the polarization states of the tristimulus wavelength of the TAC film with the slow axis OF . Therefore reverse rotation by the TAC film through the circle j centered position F will provide a polarization coin-

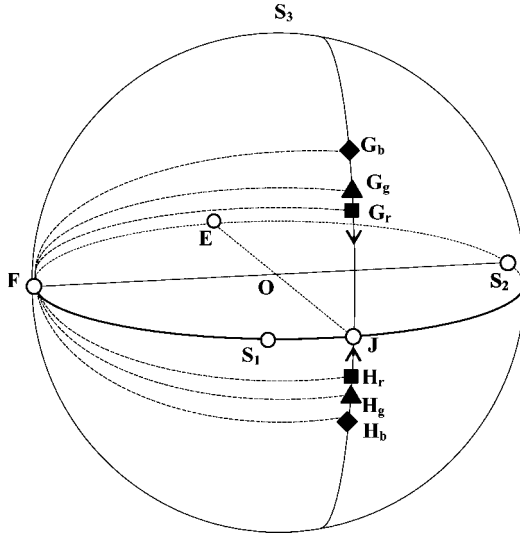


Fig. 8. Polarization state of light after passing through the $+C$ plate and upper TAC.

cidence through three wavelengths. As a result, we can expect that the final destination of the tristimulus wavelength can be matched. Retardation of the upper $+C$ plate Γ^C can also be easily achieved by applying spherical trigonometry to the spherical triangle FGH in every wavelength range:

$$\Gamma^C = \text{arc}(GJ) + \Gamma^{\text{TAC}}. \quad (5)$$

4. Discussion and Experiment

With Eqs. (4) and (5) we can easily calculate the retardations of the two A plates and the $+C$ plate in the entire wavelength range for the achromatic condition in the dark state. As shown in the equations, the solution discharges many combinations of the retardations of the A and $+C$ plates. To satisfy the practical approach, we investigated required uniaxial films in each dispersion condition. In general, we can control the dispersion of the A plate with three types, normal, flat, and reverse. By using Eqs. (4) and (5), we calculated optimized phase dispersions for the upper A and $+C$ plates in each case using the three different dispersion types of the lower A plate, respectively.

Figure 9 shows the calculated optimum phase dispersions of the upper A and $+C$ plates with three different dispersion types of the lower A plate. In terms of the upper A plate, we observe that the lower A plate, whose phase dispersions are normal and flat, respectively, permits the unusual shape of dispersed retardation for the upper A plate, as shown in Figs. 9(a) and 9(b). In practice, however, controlling formation of the dispersion of the A plate to the calculated result of Figs. 9(a) and 9(b) is very hard. Therefore it is quite difficult to apply the calculated result to the proposed horizontal-switching LC cell. In contrast, Fig. 9(c) provides a more complete and practical example for the proposed LC cell. In Fig. 9(c), the lower

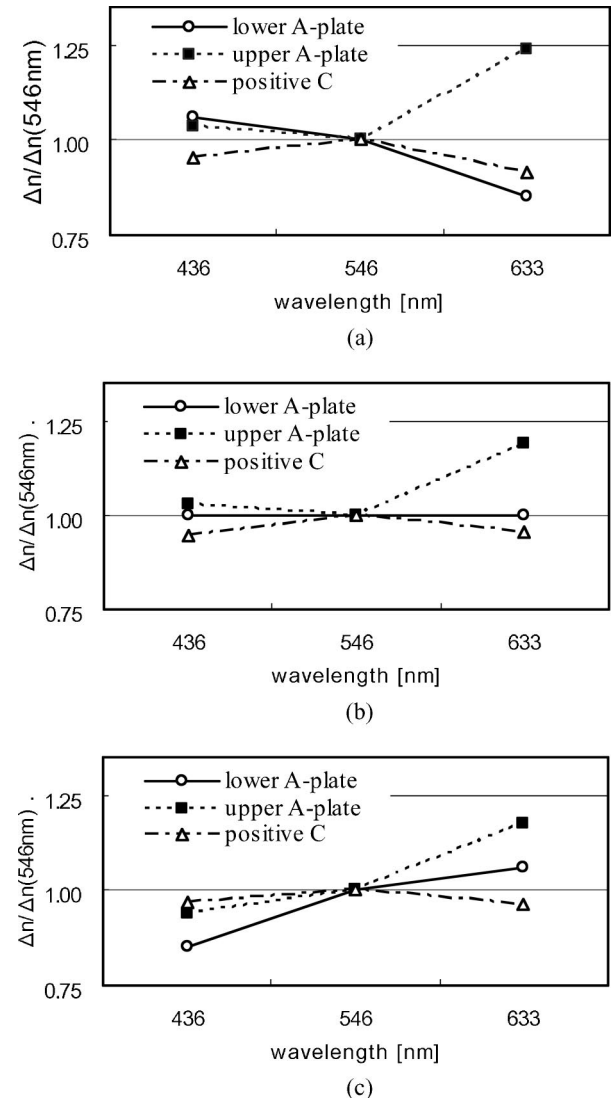


Fig. 9. Calculated material dispersion of the upper A plate and the $+C$ plate for optimization with the lower A plate: (a) with normal dispersion, (b) with flat dispersion, (c) with reverse dispersion.

A plate with the reverse dispersion discharges the calculated result, which includes the upper A plate with the reverse dispersion compared with Figs. 9(a) and 9(b). The result implies that better optical char-

Table 1. Numerical Calculation Results for Each Optical Plate in the Case of Normal Dispersion of the Lower A Plate^a

	$\Delta n/\Delta n_{(546 \text{ nm})}$		$\Delta n_{(546 \text{ nm})}$	$d [\mu\text{m}]$
	436 nm	633 nm		
TAC ($-C$ plate)	1.00	1.00	—	40
$+C$ plate	0.95	0.92	0.12049	1.2
Upper A plate	1.04	1.24	0.00142	80
LC cell	1.04	0.98	0.09720	3.4
Lower A plate	1.06	0.85	0.00145	150

^a $i,j,k,l = 1,1,2,2$ for red, $i,j,k,l = 1,2,1,2$ for green, $i,j,k,l = 2,2,2,1$ for blue.

Table 2. Numerical Calculation Results for Each Optical Plate in the Case of Flat Dispersion of the Lower A Plate^a

	$\Delta n/\Delta n_{(546 \text{ nm})}$		$\Delta n_{(546 \text{ nm})}$	$d [\mu\text{m}]$
	436 nm	633 nm		
TAC (-C plate)	1.00	1.00	—	40
+C plate	0.95	0.96	0.12049	1.2
Upper A plate	1.03	1.19	0.00142	80
LC cell	1.04	0.98	0.09720	3.4
Lower A plate	1.00	1.00	0.00145	150

^a $i,j,k,l = 1,1,2,2$ for red, $i,j,k,l = 1,2,1,2$ for green, $i,j,k,l = 2,2,2,1$ for blue.

acteristics of the horizontal-switching LC cell in the dark state can be achieved by the practical case of Fig. 9(c). Therefore the upper A plate should also possess reverse dispersed retardation. As for the +C plate, it should have unusual dispersion as shown in Fig. 9. Different from the A plate, the practical approach to apply the +C plate to the LC cell can be accomplished by coating the UV-cured LC on the substrate. Therefore it would have a normal phase dispersion because the phase dispersion of the +C plate follows the LC director. So, it may produce light leakage in the reverse dispersion wavelength range (blue area) as shown in Fig. 9. Fortunately, however, we have also found that unusual dispersion of the +C plate can be reduced by applying the A plate with reverse dispersed retardation as shown in Fig. 9.

Tables 1–3 show the calculated optimized retardations of the three uniaxial films in R, G, and B wavelengths. Based on the calculated result, we verified the improvement of the optical viewing angle of the horizontal-switching LC cell, as shown in Fig. 10. The experiment tried to follow the condition in Table 3. In Fig. 10 we confirm that the optical contrast in the diagonal direction increases by 80% compared to the conventional mode at an azimuth angle of 45° and a polar angle of 70°.

Table 3. Numerical Calculation Results for Each Optical Plate, in the Case of Reverse Dispersion of the Lower A Plate^a

	$\Delta n/\Delta n_{(546 \text{ nm})}$		$\Delta n_{(546 \text{ nm})}$	$d [\mu\text{m}]$
	436 nm	633 nm		
TAC (-C plate)	1.00	1.00	—	40
+C plate	0.97	0.96	0.12049	1.2
Upper A plate	0.94	1.18	0.00142	80
LC cell	1.04	0.98	0.09720	3.4
Lower A plate	0.85	1.06	0.00145	150

^a $i,j,k,l = 1,1,2,2$ for red, $i,j,k,l = 1,2,1,2$ for green, $i,j,k,l = 2,2,2,1$ for blue.

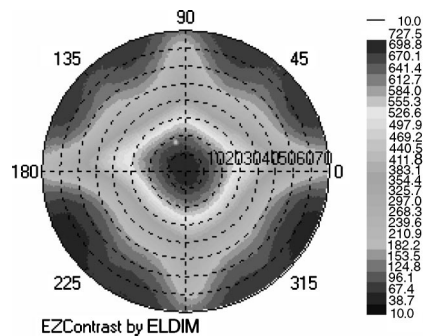


Fig. 10. Measured isocontrast contour of the proposed horizontal-switching cell, measured with EZContrast 160 D.

5. Conclusion

In conclusion we have proposed a novel optical configuration of a horizontal-switching LC cell that can improve the viewing angle in the diagonal direction. By applying a splayed LC cell and uniaxial films including two A plates and a +C plate, we could achieve symmetrically wide viewing angle characteristics. To satisfy the optimization under a practical approach, we calculated the phase dispersion of the uniaxial retardation films. As a result, we determined that the contrast ratio in the diagonal direction can be increased by 80% by applying the proposed horizontal-switching LC cell experimentally.

This work was supported in part by L. G. Philips LCD and the second Brain Korea 21 Program.

References

1. T. Ishinabe, T. Miyashita, T. Uchida, and Y. Fujimura, "A wide viewing angle polarizer and a quarter-wave plate with a wide wavelength range for extremely high quality LCDs," IDW **485**, 485–488 (2001).
2. Y. Saitoh, S. Kimura, K. Kusafuka, and H. Shimizu, "Optically compensated in-plane-switching-mode TFT-LCD panel," SID Int. Symp. Digest Tech. Papers **29**, 706–709 (1997).
3. J. E. Anderson and P. J. Bos, "Methods and concerns of compensating in-plane switching liquid crystal displays," Jpn. J. Appl. Phys. Part 1 **39**, 6388–6392 (2000).
4. J. Chen, K. H. Kim, J. J. Jyu, J. H. Souk, J. R. Kelly, and P. J. Bos, "Optimum film compensation modes for TN and VA LCDs," SID Int. Symp. Digest Tech. Papers **29**, 315–318 (1998).
5. Y. Saitoh, S. Kimura, K. Kusafuka, and H. Shimizu, "Optimum film compensation of viewing angle of contrast in in-plane-switching-mode liquid crystal display," Jpn. J. Appl. Phys. Part 1 **37**, 4822–4828 (1998).
6. T. Ishinabe, T. Miyashita, and T. Uchida, "Wide-viewing-angle polarizer with a large wavelength range," Jpn. J. Appl. Phys. Part 1 **41**, 4559–4562 (2002).
7. E. Collett, *Polarized Light* (Marcel Dekker, 1993).
8. J. E. Bigelow and R. A. Kashnow, "Poincaré sphere analysis of liquid crystal optics," Appl. Opt. **16**, 2090–2096 (1977).
9. P. Yeh and C. Gu, *Optics of Liquid Crystal Displays* (Wiley, 1999).